# A FINAL REPORT:

# THERMAL CONDUCTIVITY MEASUREMENTS IN UTAH

by

Mason C. Edwards & Davis S. Chapman

University of Utah
Department of Geology & Geophysics
June 2013

Utah Geological Survey Award 120886

July 2011-June 2013

Between September of 2011 and March of 2013, the University of Utah Geothermal Studies Lab, carried out thermal conductivity measurements on 468 samples. Samples of drill cuttings from five exploratory thermal gradient boreholes (PA-1, P-2A, PA-3, PA-5A and PA-6) were provided by the Utah Geological Survey along with cuttings from five exploratory oil & gas wells (Gronning-1, Hole-in-Rock , Pavant Butte 1, State of Utah "E" 1, and State of Utah "N" 1) . While a large number of thermal conductivity determinations have already been made on rocks from Utah, the majority of these measurements belong to Colorado Plateau rocks (Appendix A). The following report summarizes the results of new thermal conductivity determinations for Basin and Range rocks and provides context for the significance of thermal conductivity to thermal studies. Samples were measured on divided bar equipment at the University of Utah following a standard operating procedure.

In the Earth's crust, conduction is the dominant heat transmission mechanism. Fourier's Law describes conductive heat transmission from three terms where conductive heat flow ($q$), in $mWm^{-2}$, is the product of thermal conductivity ($k$), in $Wm^{-1}K^{-1}$, and the temperature gradient ($\nabla T$), in $°Ckm^{-1}$:

$$q = -k\nabla T. \quad (1)$$

From this expression we see that thermal conductivity is fundamental to understanding both terrestrial heat flow and crustal temperatures.

The primary control on thermal conductivity is bulk composition, consisting of both the matrix mineralogy and pore space. Thermal conductivity of the rock matrix can be deduced by measuring rocks of the formation of interest directly or by estimating a value based on the formation's dominant lithology. The range of matrix conductivity for common rocks and minerals is well established and observed variations range by more than a factor of eight [Beardsmore and Cull, 2001]. A single rock type, particularly sedimentary rocks, can vary by as much as a factor of three, though such large variations are not generally observed within a single formation. Figure 1 shows a compilation of thermal conductivity ranges for common rocks determined from the above sources. Due to the extent to which conductivity values vary, the most precise calculations of heat flow or temperature at depth are made with measured thermal conductivities specific to the geologic section of interest.

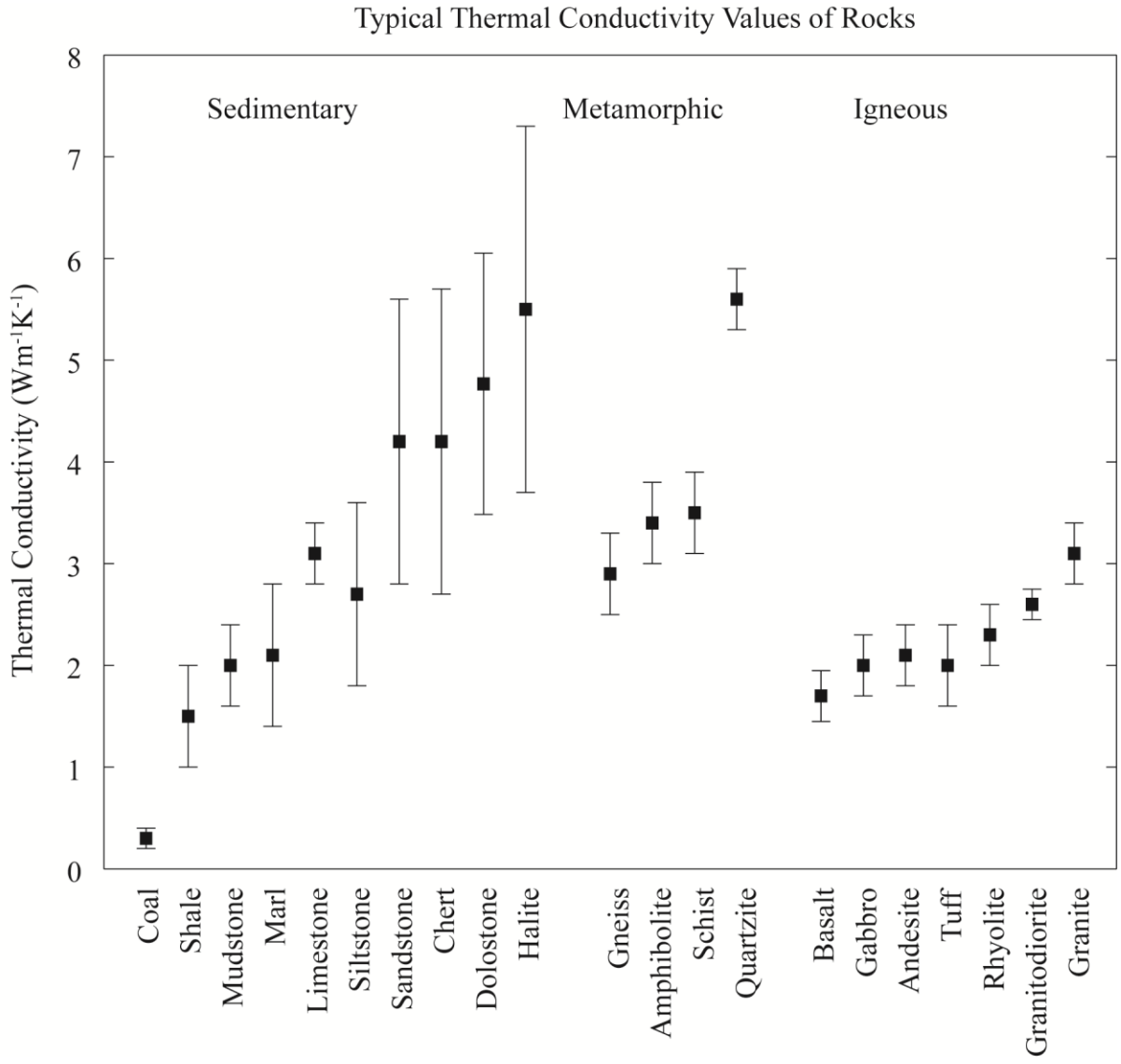


**Figure 1.** Typical thermal conductivities of common rocks. Mean values are presented as black squares and error bars indicate one standard deviation from the mean.

Measurements of thermal conductivity for this study were made by a steady state method known as the divided bar technique. The method essentially compares the one dimensional steady state temperature gradient across a sample of rock (or a cell containing water and rock chips as was done for this work) to the gradient across a reference disk with known conductivity.

Before measurement on the divided bar, drill cuttings are packed into cells which contain rock chips and water to occupy the cells' pore space. The combined dry mass of rock chips and the cell is measured. Cells are then put under vacuum and subsequently flooded with water to fill all available pore space. A second measurement, the saturated mass, is made and from this the cell porosity (which is a necessary correction factor) can be determined by relating the dry ($m_{dry}$) and wet masses ($m_{saturated}$):

$$m_{dry} + m_{water} = m_{saturated}. \quad (2)$$

The mass of water ($m_{water}$) in the cell is a function of its volume ($V_{water}$) and density ($\rho_{water}$):

$$m_{water} = V_{water} * \rho_{water}. \quad (3)$$

Since the density of water is known (1gcm$^{-3}$), these expressions can be combined and the volume of water is related to the volume of pore space ($V_{pore}$) and total cell volume ($V_{total}$) to arrive at packed cell porosity ($\varphi$):

$$V_{water} = \frac{m_{saturated} - m_{dry}}{\rho_{water}}, \quad (4)$$

$$V_{water} = m_{saturated} - m_{dry}, \quad (5)$$

$$V_{pore} = V_{water}, \quad (6)$$

$$\varphi = \frac{V_{pore}}{V_{total}}. \quad (7)$$

The setup for measuring conductivity by the divided bar method is shown schematically in Figure 2 and outlined in Sass et al. [1971], Chapman [1976], Bodell [1981] with later updates by Pribnow et al. [1995]. Temperature differences through the stack are measured at four locations bracketing two reference discs and the sample.

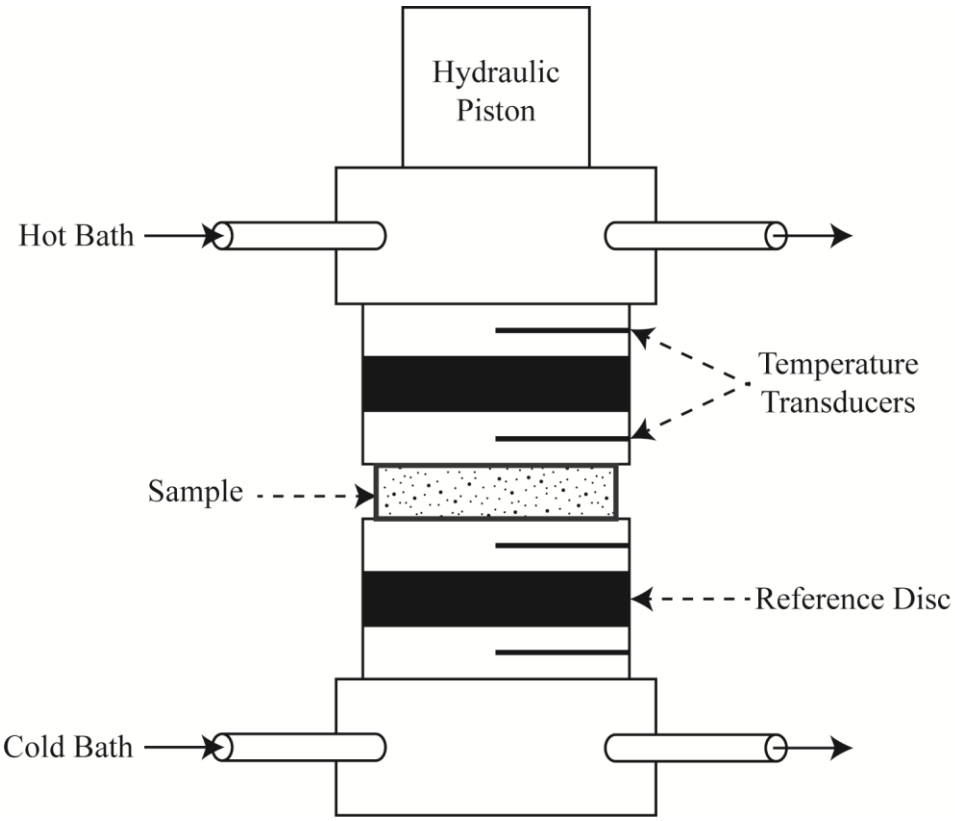


**Figure 2.** The divided bar configuration. Temperature at the top and base of the divided bar are maintained at fixed temperatures by flowing water from controlled temperature baths. Thermocouples placed in highly conductive material measure the thermal emf across the reference discs as well as the sample. A piston applies downward pressure holding all surfaces in contact, reducing the thermal contact resistance.

Assuming that no heat is lost from the system laterally, the heat flow through the sample and reference can be equated:

$$q_{ref} = k_{ref} * \nabla T_{ref}; \quad q_{sample} = k_{sample} * \nabla T_{sample}, \tag{8}$$

$$k_{ref} * \nabla T_{ref} = k_{sample} * \nabla T_{sample}, \tag{9}$$

$$k_{sample} = \frac{k_{ref} * \nabla T_{ref}}{\nabla T_{sample}}, \tag{10}$$

where $k_{ref}$ is the conductivity of the reference, and $\nabla T_{ref}$ and $\nabla T_{sample}$ are the gradients across the reference and sample respectively. The gradients and conductivity of the references are known, thus the conductivity of the sample can be calculated. The surface area of the sample

may not be the same as the surface area of the divided bar where the two are in contact. A correction for the difference in dimensions must be made:

$$k_{diam} = \frac{{d_{bar}}^2}{{d_{outer}}^2} * k_{sample}, \tag{11}$$

where ${d_{bar}}^2$ and ${d_{outer}}^2$ are the diameters of the divided bar and sample respectively. Because drill cuttings must be contained to measure on the divided bar, they are packed as rock chips into water saturated cells. When measuring cells containing rock chips and water, $k_{diam}$ includes the bulk contents of the cell as well as the cell itself. Additional corrections are required, beyond those applied to core samples, which account for the conductivity of the cell walls:

$$k_{bulk} = k_{diam} - \frac{{d_{outer}}^2 - {d_{inner}}^2}{{d_{inner}}^2} * k_{wall}, \tag{12}$$

which yields the bulk conductivity of the rock chip and water mixture in terms of $d_{outer}$ and $d_{inner}$, the diameters of the outer and inner cell walls and $k_{wall}$, the conductivity of the wall material. Finally, the rock chip conductivity can be determined from a volumetric mixing expression with two constituents, rock chips ($k_{matrix}$), water ($k_{water}$), and the total pore space ($\varphi$):

$$k_{bulk} = {k_{matrix}}^{(1-\varphi)} * {k_{water}}^{\varphi}, \tag{13}$$

which rearranges to:

$$k_{matrix} = k_{water} * \left(\frac{k_{bulk}}{k_{water}}\right)^{\frac{1}{1-\varphi}}. \tag{14}$$

The conductivity of water, $k_{water}$, is known to be 0.6 $Wm^{-1}K^{-1}$ at standard conditions, and so equation (14) provides the thermal conductivity of the rock matrix.

New divided bar conductivity measurements were made on 468 cutting samples from five shallow gradient wells and five deep oil & gas exploration wells. The five gradient holes (PA-1, P-2A, PA-3, PA-5A, and PA-6) are part of a Utah Geological Survey drilling program and are all located in the Black Rock Desert (BRD) in Millard County, Utah. These wells were selected to characterize the thermal conductivity of shallow lakebed sediments found widely throughout the

Basin and Range. Five exploration wells were selected to sample the deeper stratigraphic section of the BRD and Great Salt Lake (GSL) regions. Three wells—Gronning 1 (API: 02710423), Pavant Butte 1 (API: 02730027), and Hole-in-Rock 1 (API: 02730019)—are located in BRD and two wells—State of Utah "E" 1 (API: 01130002) and State of Utah "N" 1 (API: 04530010)—are in the GSL region. Figure 3 illustrates the locations of the ten wells.

The shallow gradient holes encountered hydrated clays and basalt. Approximate whole rock conductivities measured on 197 clay samples varied from 1.01 $Wm^{-1}K^{-1}$ to 1.67 $Wm^{-1}K^{-1}$ with a mean of 1.30 $Wm^{-1}K^{-1}$ and standard deviation 0.15 $Wm^{-1}K^{-1}$. Basalts varied between 1.94 $Wm^{-1}K^{-1}$ and 2.89 $Wm^{-1}K^{-1}$ with a mean 2.26 $Wm^{-1}K^{-1}$ and standard deviation 0.29 $Wm^{-1}K^{-1}$ for the 9 samples measured.

Conductivity measured in the deep wells varies between 1.8 $Wm^{-1}K^{-1}$ and 8.7 $Wm^{-1}K^{-1}$. The large range observed reflects the variable composition of the stratigraphic section of interest and demonstrates the significance of characterizing its conductivity. The two wells in GSL encountered Quaternary and Tertiary basin sediments, upper Paleozoic carbonates and Paleozoic metamorphosed basement, most likely the Tintic Quartzite. Measured values of conductivity are $3.32 \pm 0.62$ $Wm^{-1}K^{-1}$, $3.39 \pm 0.50$ $Wm^{-1}K^{-1}$, $3.37 \pm 0.36$ $Wm^{-1}K^{-1}$, and $6.36 \pm 1.54$ $Wm^{-1}K^{-1}$ for each respectively. The three wells in BRD logged mostly Tertiary basin sediment (mudstones, salt, and sandstone) and basalts which unconformably overlay Paleozoic carbonates and metamorphosed Paleozoic basement, most likely Prospect Mountain Quartzite, as observed by penetrations at Hole-in-the-Rock 1 and Pavant Butte 1. Conductivities measured through the stratigraphic section are $3.42 \pm 0.87$ $Wm^{-1}K^{-1}$ for the Quaternary section, $2.98 \pm 0.58$ $Wm^{-1}K^{-1}$ for the Tertiary basin fill, $4.84 \pm 1.43$ $Wm^{-1}K^{-1}$ in the Paleozoic carbonates, and $4.82 \pm 0.73$ $Wm^{-}$

$^{1}K^{-1}$ in the Prospect Mountain Quartzite. Table 1 summarizes the measured values by rock unit and Appendix B shows all thermal conductivity measurements made.

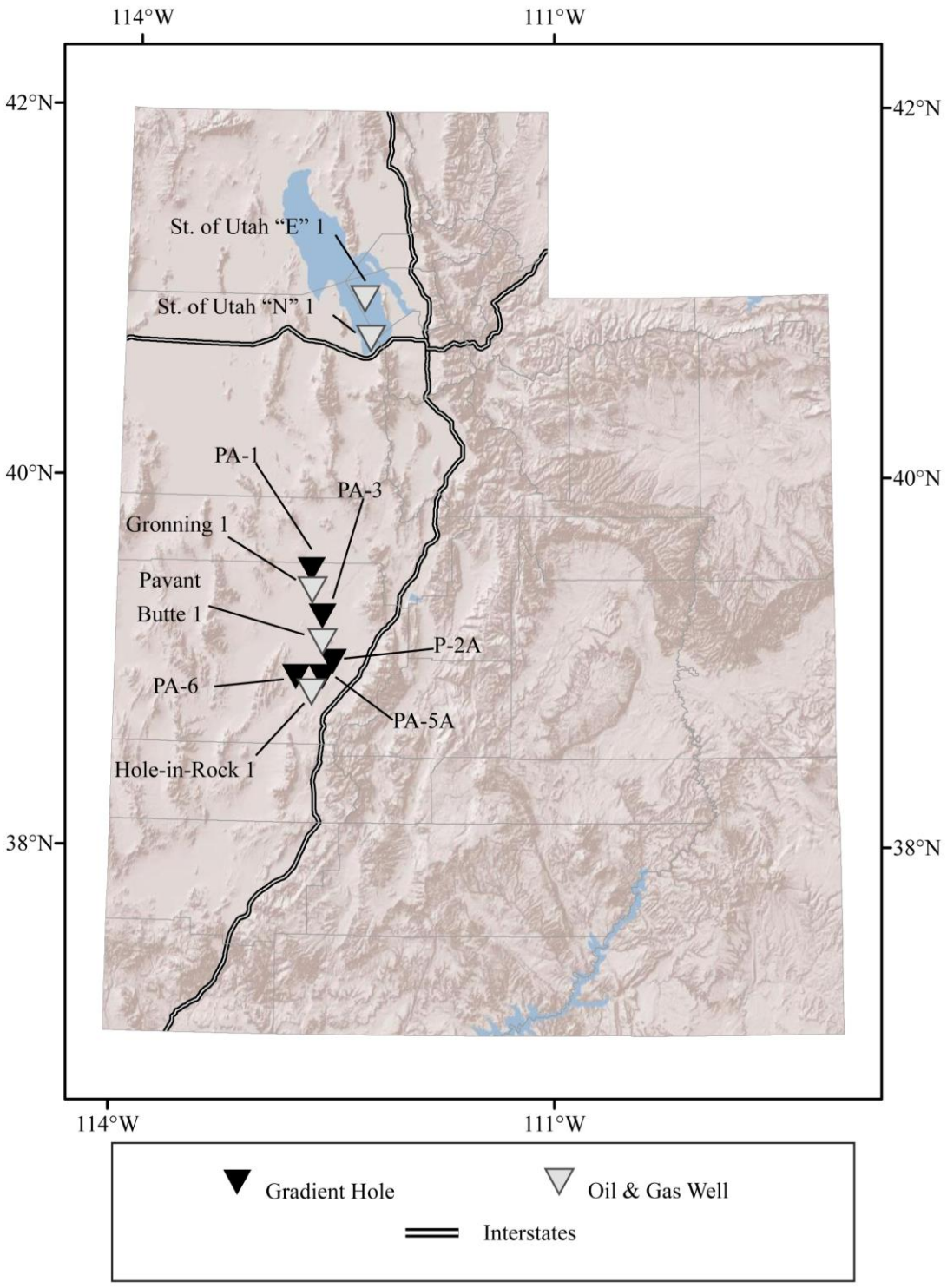


**Figure 3.** Locations of wells with new thermal conductivity measurements. White triangles indicate samples were taken from exploration wells and black triangles indicate samples were from shallow gradient holes.

**Table 1.** New thermal conductivity measurements*

| Rock Unit | Thermal Conductivity ($Wm^{-1}K^{-1}$) | Standard Deviation ($Wm^{-1}K^{-1}$) | n Samples |
|---|---|---|---|
| Quaternary lakebed sediments[1] | 1.30 | 0.15 | 197 |
| Quaternary basalts[2] | 2.26 | 0.29 | 9 |
| BRD Quaternary valley fill[2] | 3.42 | 0.87 | 24 |
| GSL Quaternary valley fill[2] | 3.32 | 0.62 | 40 |
| BRD Tertiary valley fill[2] | 2.98 | 0.58 | 123 |
| GSL Tertiary valley fill[2] | 3.39 | 0.50 | 10 |
| BRD Paleozoic carbonates[2] | 4.84 | 1.43 | 15 |
| GSL Paleozoic carbonates[2] | 3.37 | 0.36 | 8 |
| Tintic Quartzite[2] | 6.36 | 1.54 | 38 |
| Prospect Mountain Quartzite[2] | 4.82 | 0.73 | 3 |

* Conductivities measured on the divided bar.
[1]Whole rock conductivity
[2]Matrix conductivity

# APPENDIX A

**Table A1.** Existing Thermal Conductivity Measurements of Utah Rock*

| Formation | Thermal Conductivity[1] ($Wm^{-2}K^{-2}$) | σ | n Samples | Lithology | Reference |
|---|---|---|---|---|---|
| Ankareh | 3.23 | 0.25 | 15 | Sandstone | Deming and Chapman 1988[2] |
| Aspen | 2.56 | 0.06 | 17 | Shale | Deming and Chapman 1988[2] |
| Bear River | 2.98 | 0.09 | 20 | | Deming and Chapman 1988[2] |
| Carmel | 2.83 | 0.71 | 8 | Mudstone, Sandstone | Powell 1997[2] |
| Carmel | 2.88 | 0.58 | 17 | Gypsum-Limestone | Bodell and Chapman 1982[3] |
| Carmel | 2.6 | 0.38 | 6 | Mudstone | Bodell and Chapman 1982[3] |
| Carmel | 3.37 | 0.5 | 7 | Siltstone-Sandstone | Bodell and Chapman 1982[3] |
| Carmel | 1.38 | | 1 | Gypsum | Bodell and Chapman 1982[3] |
| Carmel | 3.03 | 0.09 | 3 | Limestone | Bodell and Chapman 1982[3] |
| Chinle | 4.71 | 1.3 | 8 | Siltstone-Conglomerate | Bodell and Chapman 1982[3] |
| Chinle | 3.44 | 0.21 | 2 | Siltstone | Bodell and Chapman 1982[3] |
| Chinle | 4.96 | 0.51 | 3 | Sandstone | Bodell and Chapman 1982[3] |
| Chinle | 7.14 | 0.41 | 2 | Very Coarse Sandstone | Bodell and Chapman 1982[3] |
| Chinle | 2.47 | | 1 | Conglomerate | Bodell and Chapman 1982[3] |
| Chinle, Shinarump | 7.26 | 0.97 | 4 | Coarse Sandstone | Powell 1997[2] |
| Claron | 3.68 | 0.2 | 29 | Limestone | Powell 1997[2] |
| Claron | 3.9 | 0.22 | 10 | Silty Limestone | Powell 1997[2] |
| Coconino | 4.82 | | 1 | Sandstone | Powell 1997[2] |
| Coconino | 7.55 | 0.36 | 5 | Sandstone | Bodell and Chapman 1982[3] |

**Table A1:** Continued

| Formation | Thermal Conductivity[1] ($Wm^{-2}K^{-2}$) | σ | n Samples | Lithology | Reference |
|---|---|---|---|---|---|
| Curtis | 4.08 | 0.51 | 4 | Conglomerate | Bodell and Chapman 1982[3] |
| Cutler-Rico | 3.36 | 0.5 | 15 | Sandstone-Limestone | Bodell and Chapman 1982[3] |
| Cutler-Rico | 4.02 | 0.41 | 6 | Silty Sandstone | Bodell and Chapman 1982[3] |
| Cutler-Rico | 3.03 | 0.41 | 7 | Arkose Sandstone | Bodell and Chapman 1982[3] |
| Cutler-Rico | 3.1 | 0.22 | 2 | Limestone | Bodell and Chapman 1982[3] |
| Dakota | 6.38 | | 1 | Sandstone | Bodell and Chapman 1982[3] |
| Duchesne | 4.80 | 1.3 | 51 | Sandstone | Chapman et al. 1984[2] |
| Echo Canyon | 6.43 | 0.65 | 21 | Sandstone-Conglomerate | Deming and Chapman 1988[2] |
| Elephant Canyon | 5.27 | 0.63 | 7 | Dolomite-Sandstone | Bodell and Chapman 1982[3] |
| Elephant Canyon | 5.39 | 0.42 | 4 | Dolomite | Bodell and Chapman 1982[3] |
| Elephant Canyon | 5.06 | 0.81 | 3 | Siltstone-Sandstone | Bodell and Chapman 1982[3] |
| Entrada | 4.77 | 0.74 | 2 | Sandstone | Powell 1997[2] |
| Entrada | 3.86 | 0.67 | 19 | Siltstone-Sandstone | Bodell and Chapman 1982[3] |
| Entrada | 3.17 | 0.43 | 10 | Siltstone | Bodell and Chapman 1982[3] |
| Entrada | 4.58 | 0.61 | 9 | Sandstone | Bodell and Chapman 1982[3] |
| Ferron | 4.22 | | 1 | Sandstone | Bodell and Chapman 1982[3] |
| Frontier | 2.47 | 0.67 | 42 | Sandstone-Shale | Deming and Chapman 1988[2] |
| Gannett | 3.47 | 0.19 | 45 | Limestone-Conglomerate | Deming and Chapman 1988[2] |
| Green River | 3.05 | 0.85 | 352 | Shale | Chapman et al. 1984[2] |

**Table A1:** Continued

| Formation | Thermal Conductivity[1] ($Wm^{-2}K^{-2}$) | σ | n Samples | Lithology | Reference |
|---|---|---|---|---|---|
| Guilmette | 2.73 | 0.35 | 9 | Limestone | Henrickson 2000[4] |
| Hermit | 2.66 | 0.13 | 2 | Siltstone | Powell 1997[2] |
| Hermosa | 1.63 | 0.14 | 9 | Shale | Henrickson 2000[4] |
| Hermosa | 4.78 | 0.08 | 5 | Sandstone | Henrickson 2000[4] |
| Honaker trail | 3.25 | 0.64 | 10 | Mudstone-Sandstone, Limestone | Bodell and Chapman 1982[3] |
| Honaker trail | 2.46 | 0.32 | 2 | Mudstone | Bodell and Chapman 1982[3] |
| Honaker trail | 3.99 | 0.2 | 4 | Sandstone | Bodell and Chapman 1982[3] |
| Honaker trail | 2.91 | 0.09 | 4 | Limestone | Bodell and Chapman 1982[3] |
| Jordanelle Stock | 2.10 | | | | Moran 1991[5] |
| Kaibab | 3.3 | 0.31 | 2 | Limestone | Powell 1997[2] |
| Kayenta | 5.55 | 0.54 | 14 | Silty Sandstone-Sandstone | Bodell and Chapman 1982[3] |
| Kayenta | 4.68 | 0.3 | 5 | Silty Sandstone | Bodell and Chapman 1982[3] |
| Kayenta | 6 | 0.29 | 9 | Sandstone | Bodell and Chapman 1982[3] |
| Kelvin | 3.61 | 0.70 | 128 | Shaley Sandstone | Deming and Chapman 1988[2] |
| Madison | 4.3 | 0.28 | 20 | Limestone | Deming and Chapman 1988[2] |
| Mancos | 2.48 | 0.24 | 24 | Shale | Henrickson 2000[4] |
| Mesaverde | 2.80 | 0.5 | 79 | Shaley Sandstone | Chapman et al. 1984[2] |
| Moenkopi | 2.65 | 0.24 | 21 | Mudstone | Powell 1997[2] |
| Morrison | 2.74 | | 1 | Limestone | Bodell and Chapman 1982[3] |

**Table A1:** Continued

| Formation | Thermal Conductivity[1] ($Wm^{-2}K^{-2}$) | σ | n Samples | Lithology | Reference |
|---|---|---|---|---|---|
| Navajo | 6.91 | 0.51 | 17 | Sandstone | Powell 1997[2] |
| Navajo | 5.42 | 0.72 | 24 | Silty Sandstone-Sandstone | Bodell and Chapman 1982[3] |
| Navajo | 4.16 | 0.42 | 5 | Silty Sandstone | Bodell and Chapman 1982[3] |
| Navajo | 5.79 | 0.66 | 19 | Sandstone | Bodell and Chapman 1982[3] |
| Nugget | 6.13 | 0.22 | 14 | Sandstone | Deming and Chapman 1988[2] |
| Nugget | 3.73 | 0.66 | 24 | Silty-Sandstone | Deming and Chapman 1988[2] |
| pC | 3.67 | 0.34 | 9 | Gneiss | Powell 1997[2] |
| Phosphoria | 4.81 | 0.17 | 16 | | Deming and Chapman 1988[2] |
| Pruess | 3.33 | 0.12 | 43 | | Deming and Chapman 1988[2] |
| Qal | 3.00 | | | | Moran 1991[5] |
| Qb | 1.63 | 0.1 | 6 | Basalt | Powell 1997[2] |
| Quat Landslide | 2.10 | | | | Moran 1991[5] |
| Redwall | 4.94 | 0.18 | 2 | Dolomite | Bodell and Chapman 1982[3] |
| Sevy | 6.53 | | 1 | Dolomite | Henrickson 2000[4] |
| Simonson | 2.98 | 0.17 | 9 | Limestone | Henrickson 2000[4] |
| Straight Cliffs | 3.32 | 0.52 | 3 | Sandstone | Powell 1997[2] |
| Stump-Pruess | 3.46 | 0.61 | 52 | | Deming and Chapman 1988[2] |
| Summerville | 4.2 | | 1 | Siltstone | Bodell and Chapman 1982[3] |
| Thaynes | 4.05 | 0.13 | 20 | | Deming and Chapman 1988[2] |

**Table A1:** Continued

| Formation | Thermal Conductivity[1] ($Wm^{-2}K^{-2}$) | σ | n Samples | Lithology | Reference |
|---|---|---|---|---|---|
| Tm v | 2.14 | 0.06 | 3 | Rhyolite Porphyry | Powell 1997[2] |
| Tm v | 1.87 | 0.15 | 6 | Trachyte Porphyry | Powell 1997[2] |
| Tm v | 2.02 | 0.16 | 9 | Andesite Porphyry | Powell 1997[2] |
| Toroweap | 3.88 | 0.16 | 3 | Silty Limestone | Powell 1997[2] |
| Tropic, Dakota | 2.29 | | 2 | Silty Claystone | Powell 1997[2] |
| Twin Creek | 2.68 | 0.35 | 82 | | Deming and Chapman 1988[2] |
| Uinta | 3.22 | 0.5 | 199 | | Chapman et al. 1984[2] |
| Upper Moenkopi | 3.37 | 0.4 | 18 | Mudstone, Siltstone | Powell 1997[2] |
| Wasatch | 2.58 | 0.37 | 171 | | Chapman et al. 1984[2] |
| Weber | 6.03 | 0.24 | 20 | | Deming and Chapman 1988[2] |
| Weber | 4.53 | | | Quartzite | Moran 1991[5] |
| Wingate | 5.24 | 0.37 | 17 | Sandstone | Bodell and Chapman 1982[3] |
| Woodside | 2.35 | | | Shale | Moran 1991[5] |
| Woodside-Dinwoody | 3.42 | 0.05 | 20 | | Deming and Chapman 1988[2] |

*Thermal conductivities measured in the University of Utah Thermal Lab on Colorado Plateau and Basin and Range rocks.
[1]Conductivities listed for cuttings represent matrix thermal conductivity while values listed for core represent whole rock value.
[2]Conductivities from cuttings measured on the divided bar.
[3]Conductivities from core measured on the divided bar.
[4]Conductivities from cuttings measured on the divided bar and whole rock measured by TK-04.
[5]Conductivities from cuttings and core measured on the divided bar.

# APPENDIX B

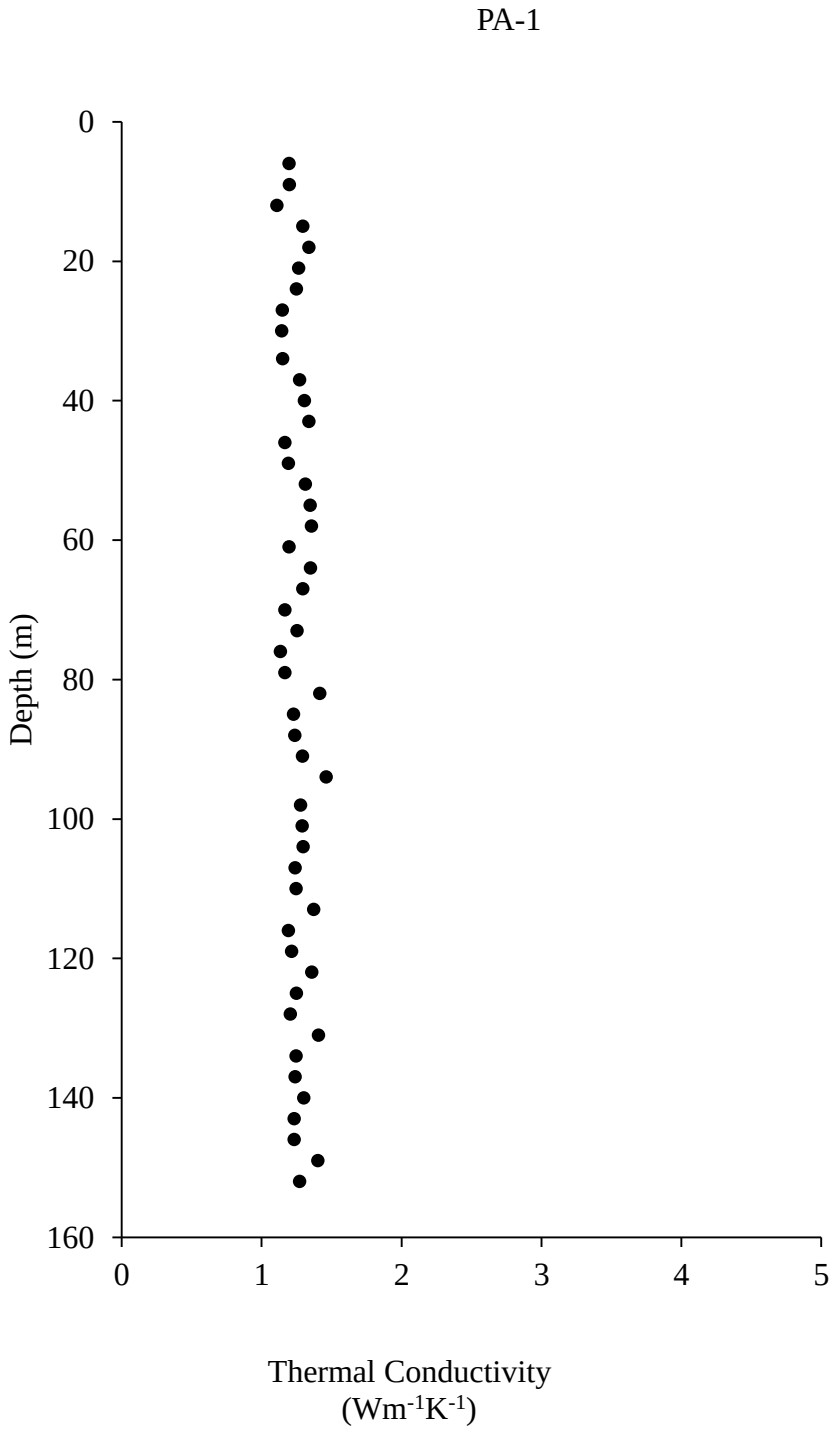


**Figure B1.** Thermal conductivities from PA-1.

**Table B1.** Thermal conductivity measurements for PA-1*

| Depth (m) | Thermal Conductivity[w] ($Wm^{-1}K^{-1}$) | Depth (m) | Thermal Conductivity[w] ($Wm^{-1}K^{-1}$) |
|---|---|---|---|
| 6.1 | 1.20 | 112.8 | 1.37 |
| 9.1 | 1.20 | 115.8 | 1.19 |
| 12.2 | 1.11 | 118.9 | 1.21 |
| 15.2 | 1.29 | 121.9 | 1.36 |
| 18.3 | 1.34 | 125 | 1.25 |
| 21.3 | 1.27 | 128 | 1.21 |
| 24.4 | 1.25 | 131.1 | 1.41 |
| 27.4 | 1.15 | 134.1 | 1.25 |
| 30.5 | 1.14 | 137.2 | 1.24 |
| 33.5 | 1.15 | 140.2 | 1.30 |
| 36.6 | 1.27 | 143.3 | 1.23 |
| 39.6 | 1.31 | 146.3 | 1.23 |
| 42.7 | 1.34 | 149.4 | 1.40 |
| 45.7 | 1.17 | 152.4 | 1.27 |
| 48.8 | 1.19 | | |
| 51.8 | 1.31 | | |
| 54.9 | 1.35 | | |
| 57.9 | 1.36 | | |
| 61 | 1.20 | | |
| 64 | 1.35 | | |
| 67.1 | 1.30 | | |
| 70.1 | 1.17 | | |
| 73.2 | 1.25 | | |
| 76.2 | 1.13 | | |
| 79.2 | 1.17 | | |
| 82.3 | 1.42 | | |
| 85.3 | 1.23 | | |
| 88.4 | 1.24 | | |
| 91.4 | 1.29 | | |
| 94.5 | 1.46 | | |
| 97.5 | 1.28 | | |
| 100.6 | 1.29 | | |
| 103.6 | 1.30 | | |
| 106.7 | 1.24 | | |
| 109.7 | 1.25 | | |

*Thermal conductivity measured on divided bar. [w]Approximate whole rock conductivity.

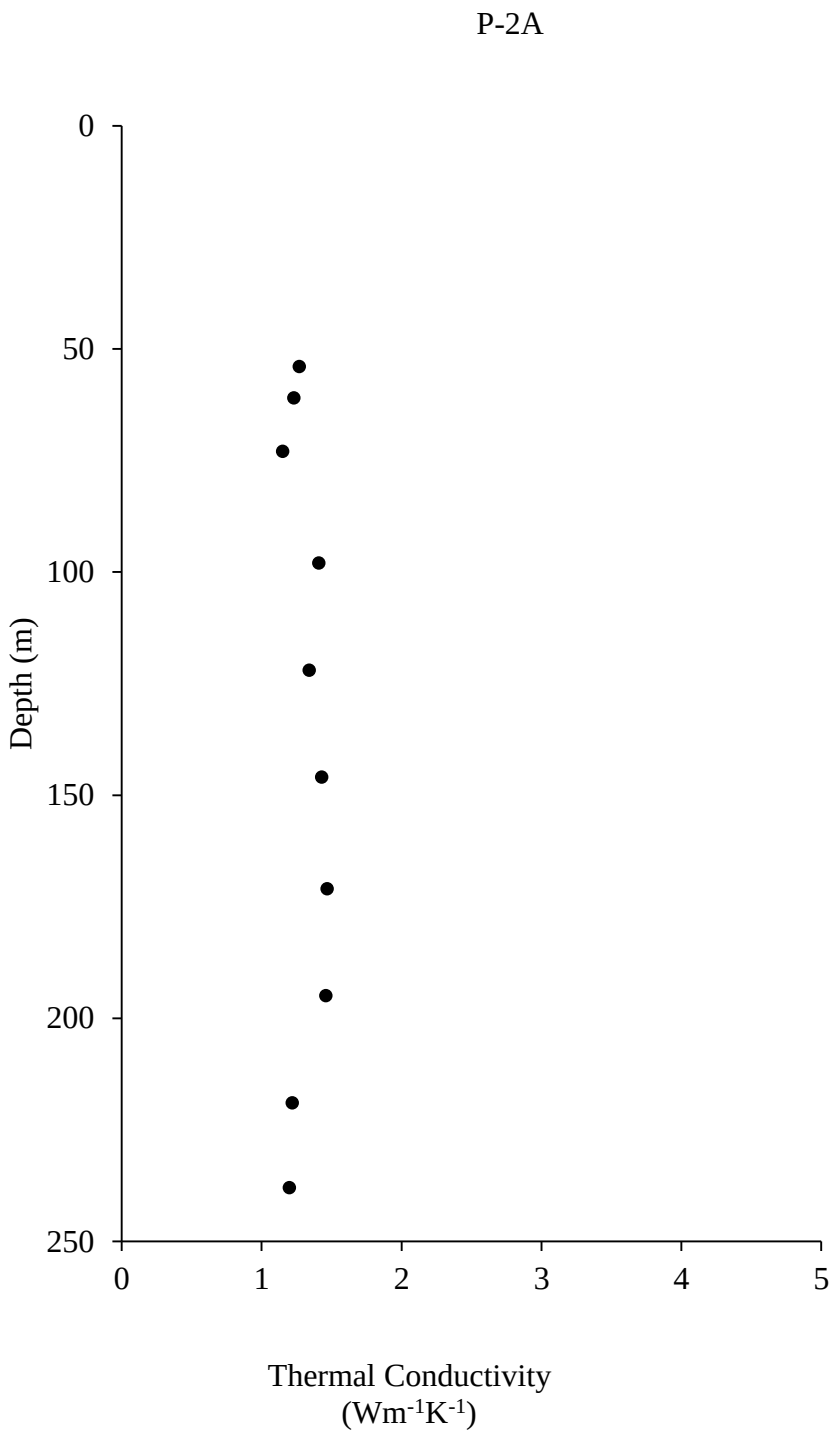


**Figure B2.** Thermal conductivities from P-2A.

**Table B2.** Thermal conductivity measurements for P-2A*

| Depth (m) | Thermal Conductivity[w] ($Wm^{-1}K^{-1}$) |
|---|---|
| 54 | 1.27 |
| 61 | 1.23 |
| 73 | 1.15 |
| 98 | 1.41 |
| 122 | 1.34 |
| 146 | 1.43 |
| 171 | 1.47 |
| 195 | 1.46 |
| 219 | 1.22 |
| 238 | 1.20 |

*Thermal conductivity measured on divided bar. [w]Approximate whole rock conductivity.

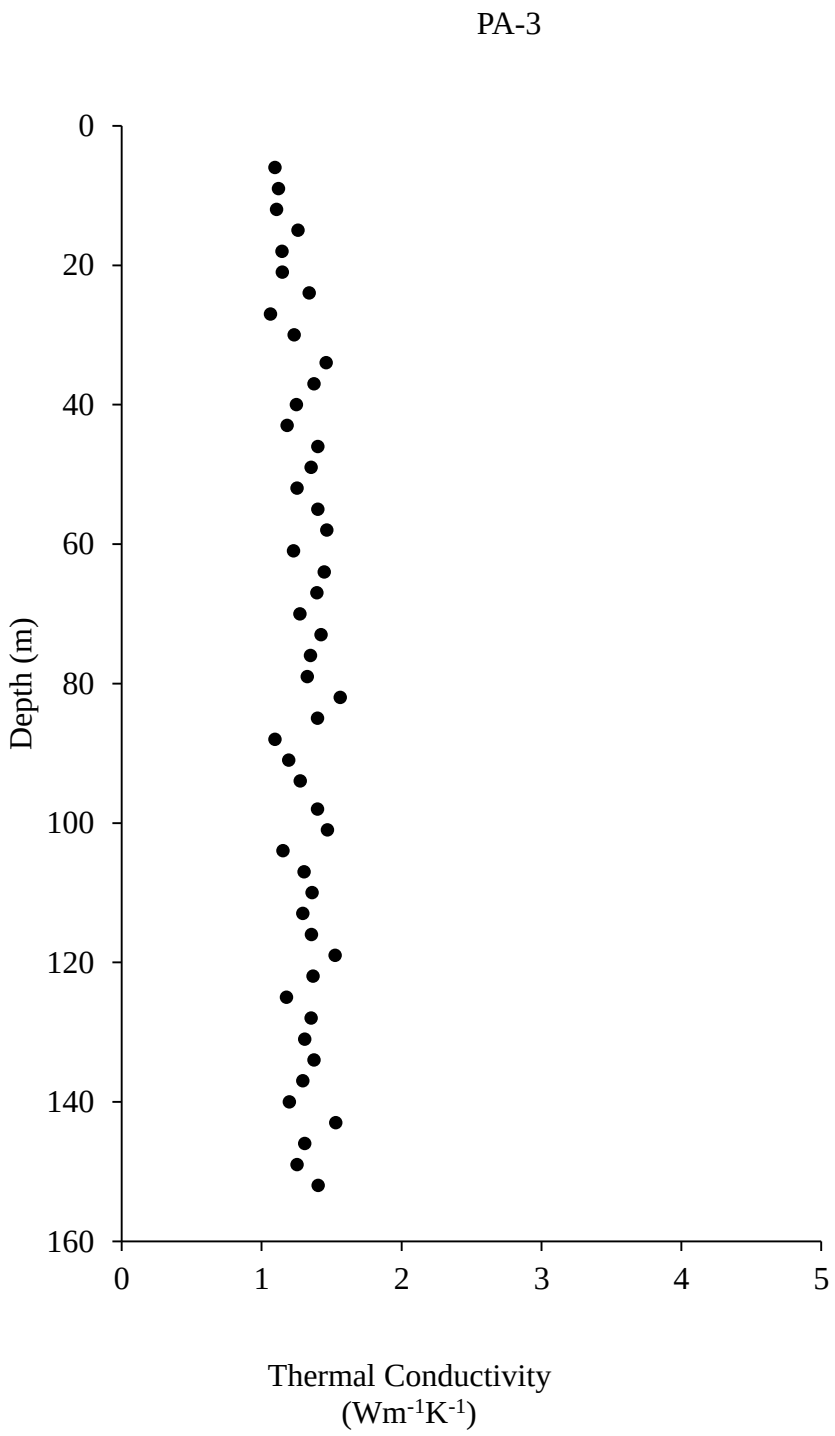


**Figure B3.** Thermal conductivities from PA-3.

**Table B3.** Thermal conductivity measurements for PA-3*

| Depth (m) | Thermal Conductivity[w] ($Wm^{-1}K^{-1}$) | Depth (m) | Thermal Conductivity[w] ($Wm^{-1}K^{-1}$) |
|---|---|---|---|
| 6.1 | 1.10 | 112.8 | 1.30 |
| 9.1 | 1.12 | 115.8 | 1.36 |
| 12.2 | 1.11 | 118.9 | 1.53 |
| 15.2 | 1.26 | 121.9 | 1.37 |
| 18.3 | 1.15 | 125 | 1.18 |
| 21.3 | 1.15 | 128 | 1.35 |
| 24.4 | 1.34 | 131.1 | 1.31 |
| 27.4 | 1.06 | 134.1 | 1.37 |
| 30.5 | 1.23 | 137.2 | 1.30 |
| 33.5 | 1.46 | 140.2 | 1.20 |
| 36.6 | 1.37 | 143.3 | 1.53 |
| 39.6 | 1.25 | 146.3 | 1.31 |
| 42.7 | 1.18 | 149.4 | 1.26 |
| 45.7 | 1.40 | 152.4 | 1.40 |
| 48.8 | 1.35 | | |
| 51.8 | 1.25 | | |
| 54.9 | 1.40 | | |
| 57.9 | 1.47 | | |
| 61 | 1.23 | | |
| 64 | 1.45 | | |
| 67.1 | 1.40 | | |
| 70.1 | 1.27 | | |
| 73.2 | 1.42 | | |
| 76.2 | 1.35 | | |
| 79.2 | 1.33 | | |
| 82.3 | 1.56 | | |
| 85.3 | 1.40 | | |
| 88.4 | 1.10 | | |
| 91.4 | 1.19 | | |
| 94.5 | 1.28 | | |
| 97.5 | 1.40 | | |
| 100.6 | 1.47 | | |
| 103.6 | 1.15 | | |
| 106.7 | 1.30 | | |
| 109.7 | 1.36 | | |

*Thermal conductivity measured on divided bar. [w]Approximate whole rock conductivity.

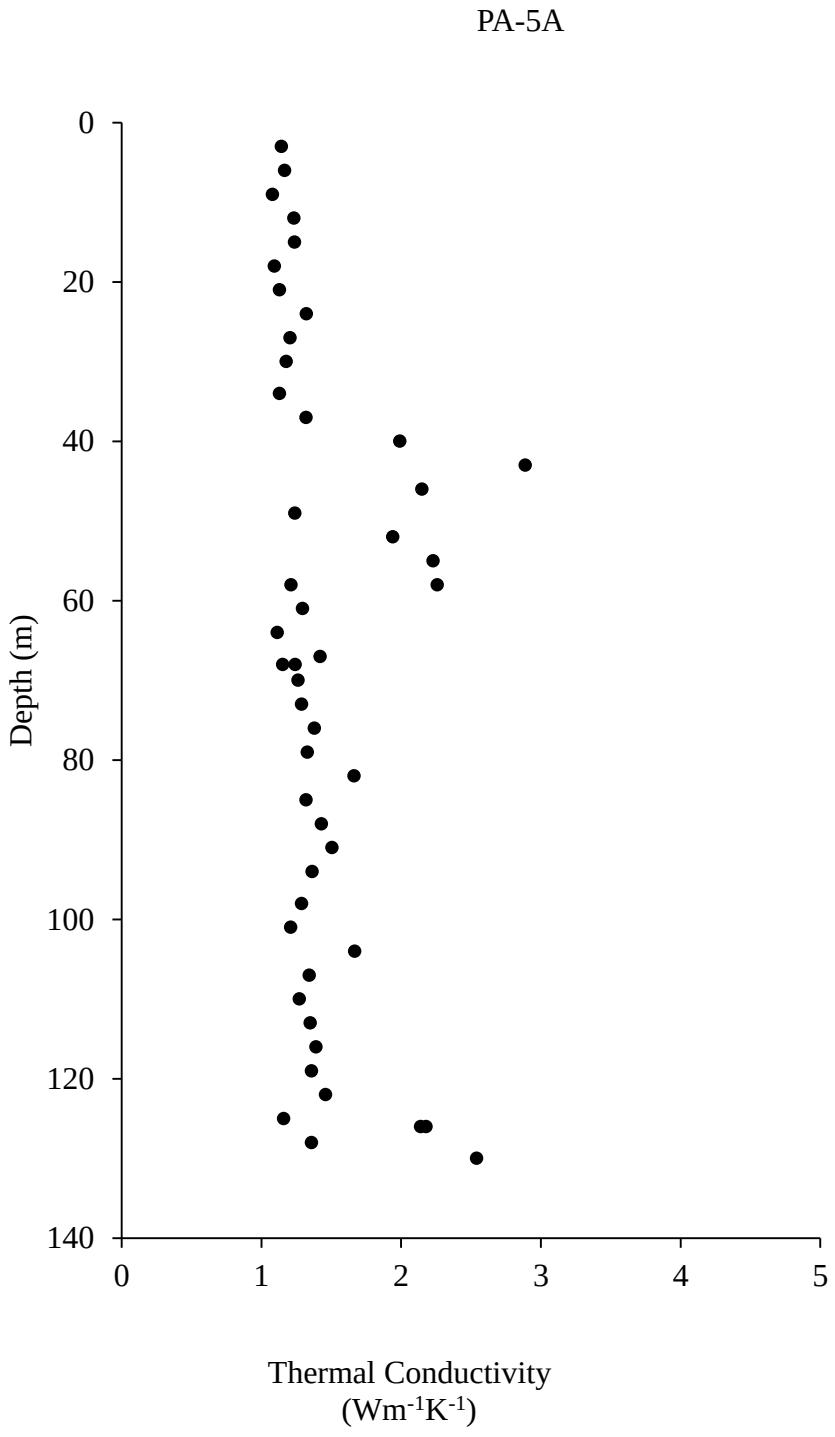


**Figure B4.** Thermal conductivities from PA-5A.

**Table B4.** Thermal conductivity measurements for PA-5A*

| Depth (m) | Thermal Conductivity ($Wm^{-1}K^{-1}$) | Depth (m) | Thermal Conductivity ($Wm^{-1}K^{-1}$) |
|---|---|---|---|
| 3 | 1.14 [w] | 100.6 | 1.21[w] |
| 6.1 | 1.17[w] | 103.6 | 1.67[w] |
| 9.1 | 1.08[w] | 106.7 | 1.34[w] |
| 12.2 | 1.23[w] | 109.7 | 1.27[w] |
| 15.2 | 1.24[w] | 112.8 | 1.35[w] |
| 18.3 | 1.09[w] | 115.8 | 1.39[w] |
| 21.3 | 1.13[w] | 118.9 | 1.36[w] |
| 24.4 | 1.32[w] | 121.9 | 1.46[w] |
| 27.4 | 1.21[w] | 125 | 1.16[w] |
| 30.5 | 1.18[w] | 125.6 | 2.18[m] |
| 33.5 | 1.13[w] | 125.6 | 2.14[m] |
| 36.6 | 1.32[w] | 128 | 1.36[w] |
| 39.6 | 1.99[m] | 129.8 | 2.54[m] |
| 42.7 | 2.89[m] | | |
| 45.7 | 2.15[m] | | |
| 48.8 | 1.24[w] | | |
| 51.8 | 1.94[m] | | |
| 54.9 | 2.23[m] | | |
| 57.9 | 2.26[m] | | |
| 57.9 | 1.21[w] | | |
| 61 | 1.30[w] | | |
| 64 | 1.11[w] | | |
| 67.1 | 1.42[w] | | |
| 68 | 1.24[w] | | |
| 68 | 1.15[w] | | |
| 70.1 | 1.26[w] | | |
| 73.2 | 1.29[w] | | |
| 76.2 | 1.38[w] | | |
| 79.2 | 1.33[w] | | |
| 82.3 | 1.66[w] | | |
| 85.3 | 1.32[w] | | |
| 88.4 | 1.43[w] | | |
| 91.4 | 1.51[w] | | |
| 94.5 | 1.36[w] | | |
| 97.5 | 1.29[w] | | |

*Thermal conductivity measured on divided bar. [w]Approximate whole rock conductivity. [m]Matrix conductivity.

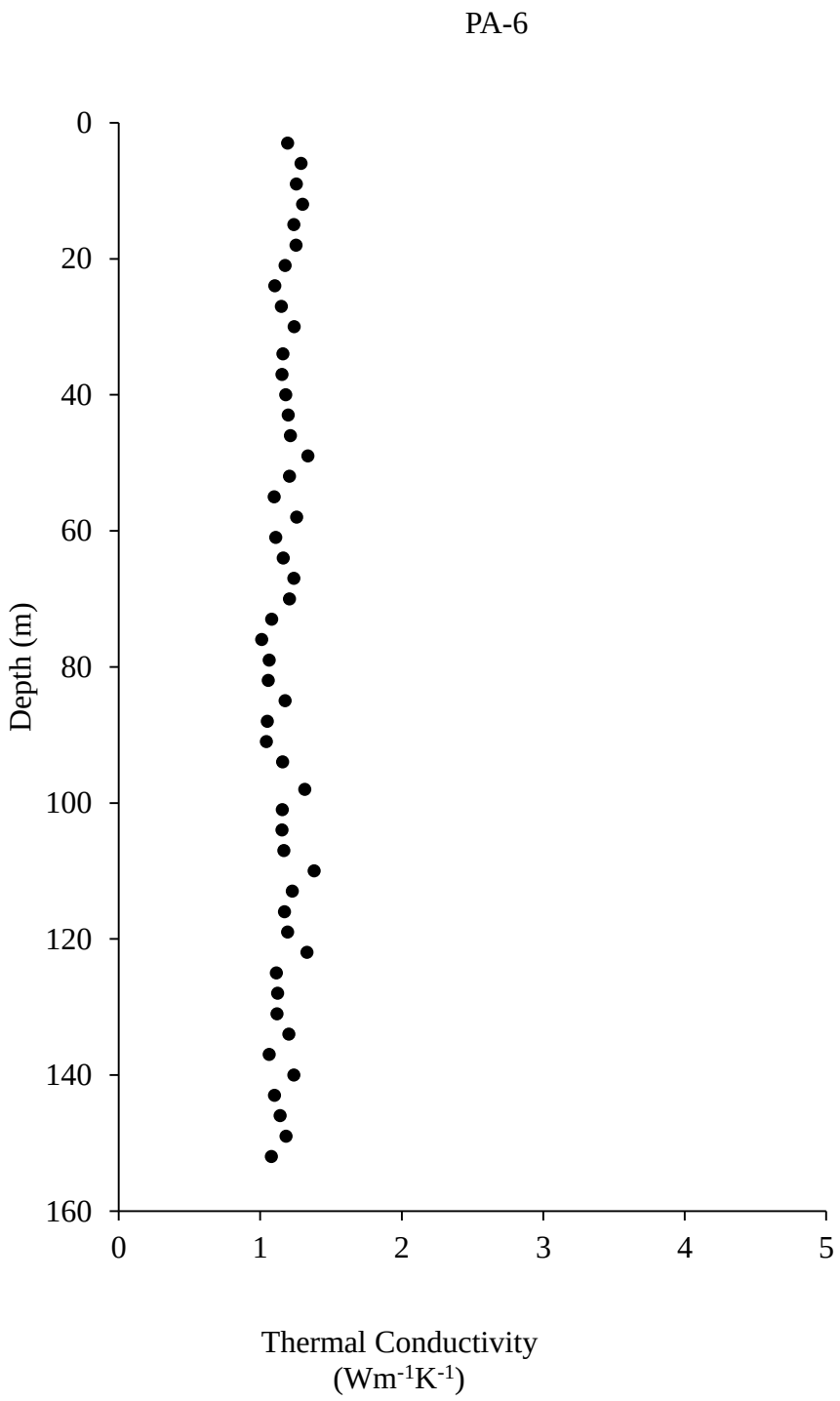


**Figure B5.** Thermal conductivities from PA-6.

**Table B5.** Thermal conductivity measurements for PA-6*

| Depth (m) | Thermal Conductivity[w] ($Wm^{-1}K^{-1}$) | Depth (m) | Thermal Conductivity[w] ($Wm^{-1}K^{-1}$) |
|---|---|---|---|
| 3 | 1.19 | 109.7 | 1.38 |
| 6.1 | 1.29 | 112.8 | 1.23 |
| 9.1 | 1.26 | 115.8 | 1.17 |
| 12.2 | 1.30 | 118.9 | 1.20 |
| 15.2 | 1.24 | 121.9 | 1.33 |
| 18.3 | 1.25 | 125 | 1.11 |
| 21.3 | 1.18 | 128 | 1.12 |
| 24.4 | 1.10 | 131.1 | 1.12 |
| 27.4 | 1.15 | 134.1 | 1.20 |
| 30.5 | 1.24 | 137.2 | 1.06 |
| 33.5 | 1.16 | 140.2 | 1.24 |
| 36.6 | 1.16 | 143.3 | 1.10 |
| 39.6 | 1.18 | 146.3 | 1.14 |
| 42.7 | 1.20 | 149.4 | 1.18 |
| 45.7 | 1.21 | 152.4 | 1.08 |
| 48.8 | 1.34 | | |
| 51.8 | 1.21 | | |
| 54.9 | 1.10 | | |
| 57.9 | 1.26 | | |
| 61 | 1.11 | | |
| 64 | 1.16 | | |
| 67.1 | 1.24 | | |
| 70.1 | 1.21 | | |
| 73.2 | 1.08 | | |
| 76.2 | 1.01 | | |
| 79.2 | 1.06 | | |
| 82.3 | 1.06 | | |
| 85.3 | 1.18 | | |
| 88.4 | 1.05 | | |
| 91.4 | 1.05 | | |
| 94.5 | 1.16 | | |
| 97.5 | 1.31 | | |
| 100.6 | 1.16 | | |
| 103.6 | 1.15 | | |
| 106.7 | 1.17 | | |

*Thermal conductivity measured on divided bar. [w]Approximate whole rock conductivity.

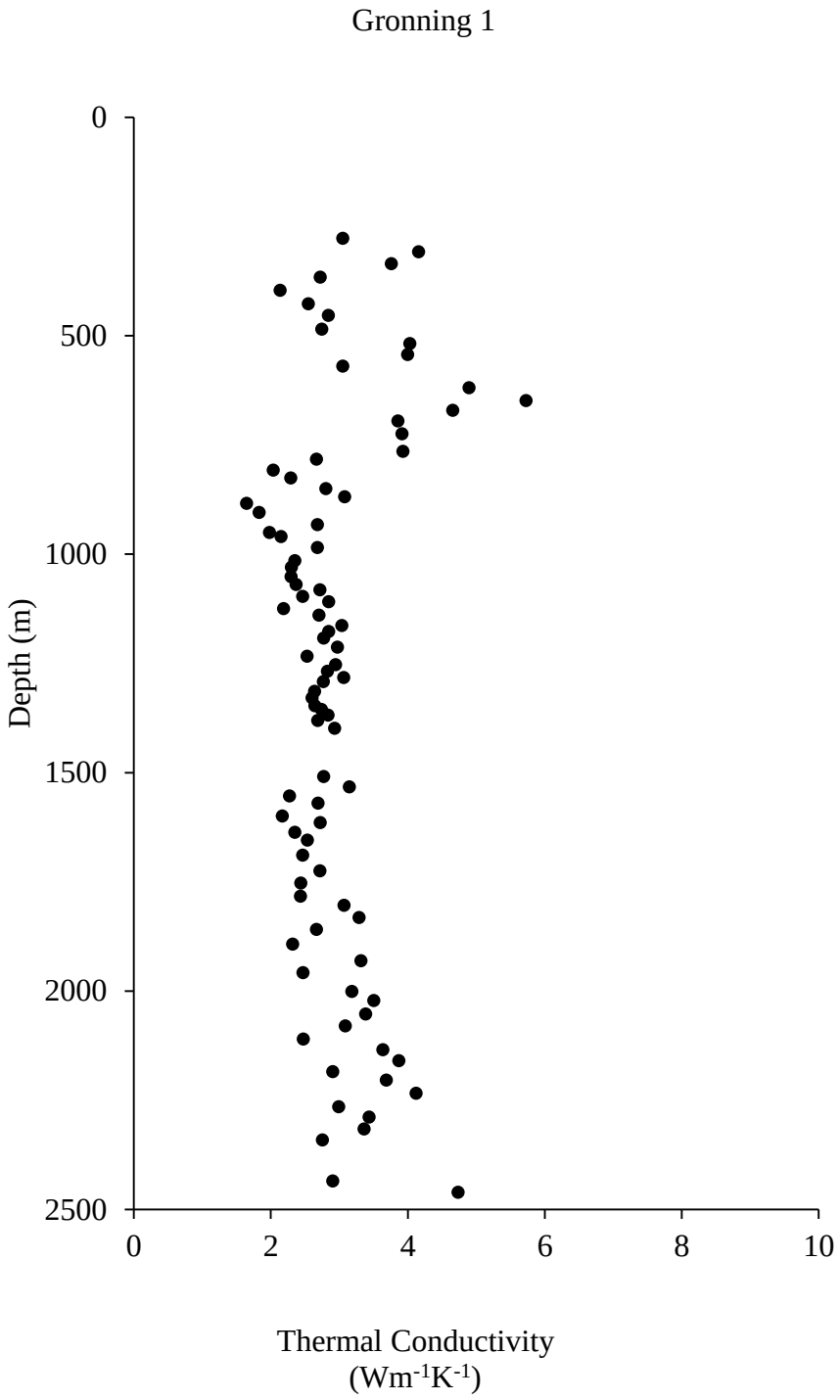


**Figure B6.** Thermal conductivities from Gronning 1.

**Table B6.** Thermal conductivity measurements for Gronning 1*

| Depth (m) | Thermal Conductivity$^{m}$ ($Wm^{-1}K^{-1}$) | Depth (m) | Thermal Conductivity$^{m}$ ($Wm^{-1}K^{-1}$) | Depth (m) | Thermal Conductivity$^{m}$ ($Wm^{-1}K^{-1}$) |
|---|---|---|---|---|---|
| 277 | 3.05 | 1125 | 2.19 | 1958 | 2.47 |
| 308 | 4.16 | 1140 | 2.70 | 2001 | 3.18 |
| 335 | 3.76 | 1164 | 3.04 | 2022 | 3.51 |
| 366 | 2.73 | 1177 | 2.85 | 2053 | 3.39 |
| 396 | 2.14 | 1192 | 2.77 | 2080 | 3.09 |
| 427 | 2.55 | 1213 | 2.98 | 2110 | 2.48 |
| 454 | 2.84 | 1234 | 2.53 | 2135 | 3.64 |
| 485 | 2.75 | 1253 | 2.95 | 2160 | 3.87 |
| 518 | 4.03 | 1268 | 2.83 | 2185 | 2.91 |
| 543 | 4.00 | 1283 | 3.07 | 2204 | 3.69 |
| 570 | 3.05 | 1292 | 2.77 | 2234 | 4.12 |
| 619 | 4.90 | 1314 | 2.64 | 2265 | 2.99 |
| 649 | 5.73 | 1329 | 2.60 | 2289 | 3.44 |
| 671 | 4.66 | 1347 | 2.65 | 2316 | 3.37 |
| 695 | 3.86 | 1356 | 2.74 | 2341 | 2.76 |
| 725 | 3.92 | 1369 | 2.84 | 2435 | 2.90 |
| 765 | 3.93 | 1381 | 2.69 | 2461 | 4.73 |
| 783 | 2.67 | 1399 | 2.93 | | |
| 808 | 2.04 | 1509 | 2.77 | | |
| 826 | 2.29 | 1533 | 3.15 | | |
| 850 | 2.81 | 1554 | 2.28 | | |
| 869 | 3.08 | 1570 | 2.69 | | |
| 884 | 1.65 | 1600 | 2.17 | | |
| 905 | 1.83 | 1615 | 2.73 | | |
| 933 | 2.68 | 1637 | 2.35 | | |
| 951 | 1.98 | 1655 | 2.54 | | |
| 960 | 2.15 | 1689 | 2.47 | | |
| 985 | 2.68 | 1725 | 2.72 | | |
| 1015 | 2.35 | 1753 | 2.44 | | |
| 1030 | 2.30 | 1783 | 2.44 | | |
| 1052 | 2.30 | 1804 | 3.07 | | |
| 1070 | 2.37 | 1832 | 3.29 | | |
| 1082 | 2.72 | 1859 | 2.67 | | |
| 1097 | 2.47 | 1893 | 2.32 | | |
| 1109 | 2.85 | 1931 | 3.32 | | |

*Thermal conductivity measured on divided bar. $^{m}$Matrix conductivity.

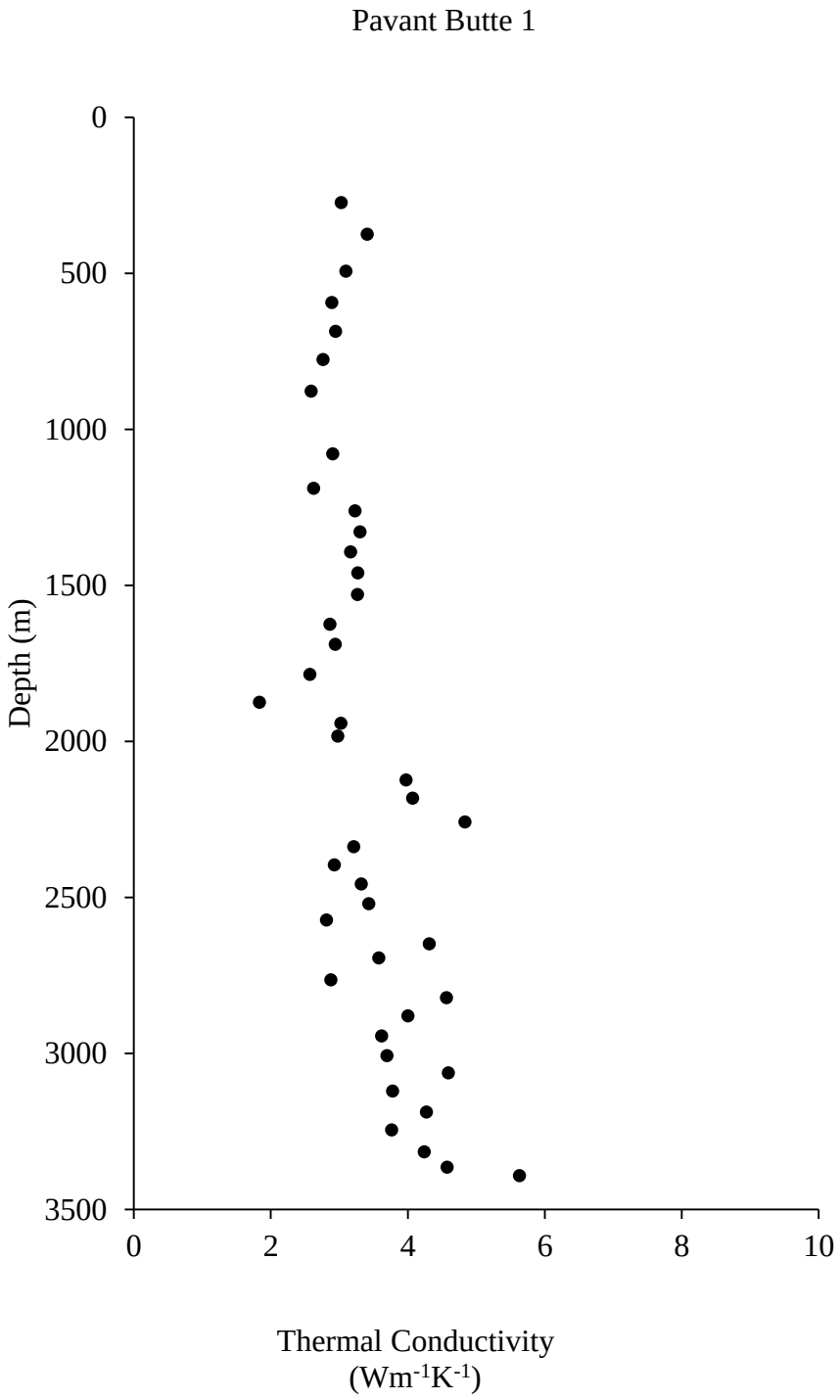


**Figure B7.** Thermal conductivities from Pavant Butte 1.

**Table B7.** Thermal conductivity measurements for Pavant Butte 1*

| Depth (m) | Thermal Conductivity$^{m}$ ($Wm^{-1}K^{-1}$) | Depth (m) | Thermal Conductivity$^{m}$ ($Wm^{-1}K^{-1}$) |
|---|---|---|---|
| 274 | 3.03 | 3063 | 4.59 |
| 375 | 3.41 | 3121 | 3.78 |
| 494 | 3.10 | 3188 | 4.27 |
| 594 | 2.89 | 3246 | 3.77 |
| 686 | 2.95 | 3316 | 4.24 |
| 777 | 2.76 | 3365 | 4.58 |
| 878 | 2.59 | 3392 | 5.63 |
| 1079 | 2.91 | | |
| 1189 | 2.63 | | |
| 1262 | 3.23 | | |
| 1329 | 3.30 | | |
| 1393 | 3.17 | | |
| 1460 | 3.27 | | |
| 1530 | 3.27 | | |
| 1625 | 2.87 | | |
| 1689 | 2.94 | | |
| 1786 | 2.57 | | |
| 1875 | 1.84 | | |
| 1942 | 3.02 | | |
| 1984 | 2.98 | | |
| 2124 | 3.98 | | |
| 2182 | 4.07 | | |
| 2259 | 4.84 | | |
| 2338 | 3.21 | | |
| 2396 | 2.93 | | |
| 2457 | 3.32 | | |
| 2521 | 3.43 | | |
| 2573 | 2.81 | | |
| 2649 | 4.32 | | |
| 2694 | 3.58 | | |
| 2765 | 2.88 | | |
| 2822 | 4.57 | | |
| 2880 | 4.00 | | |
| 2944 | 3.62 | | |
| 3008 | 3.7 | | |

*Thermal conductivity measured on divided bar. $^{m}$Matrix conductivity.

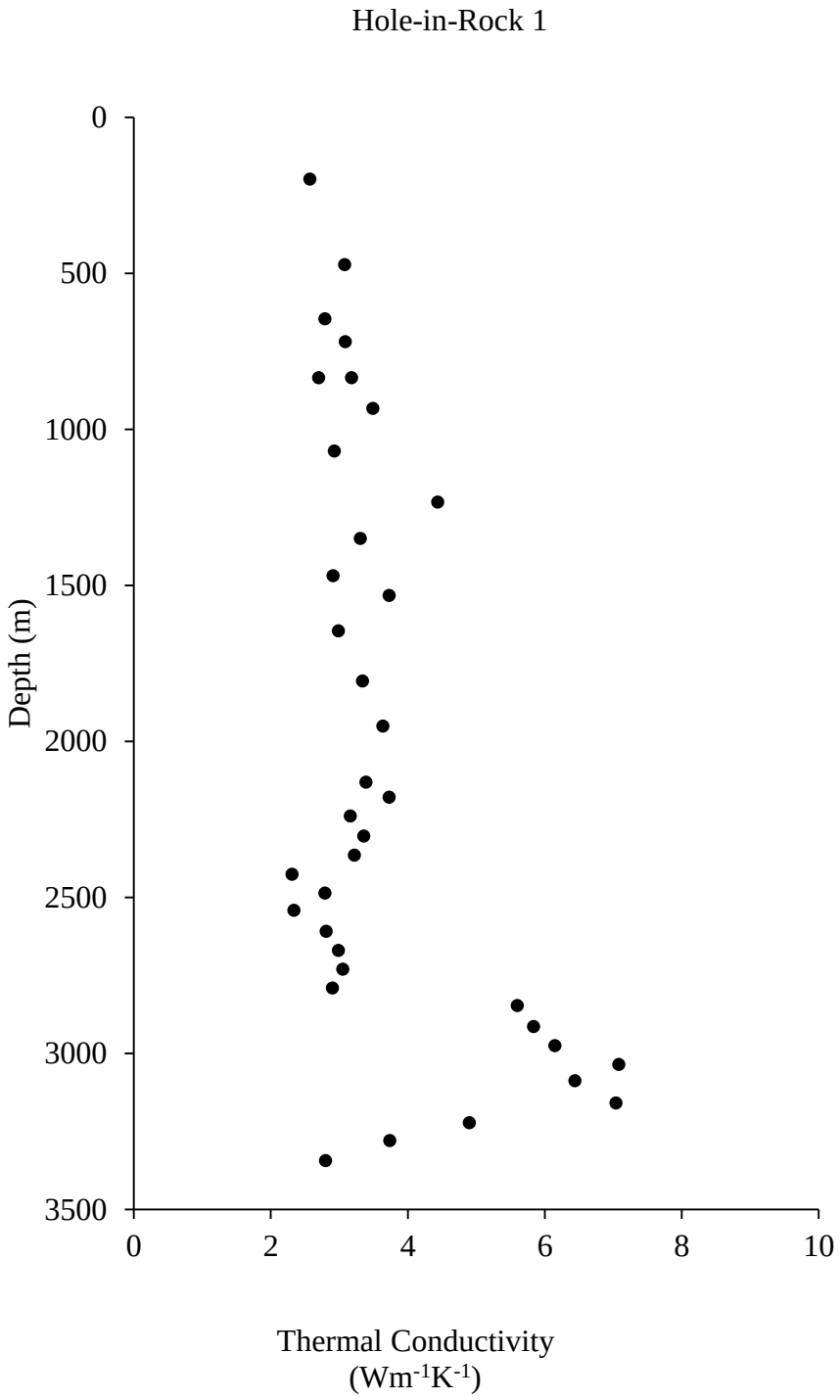


**Figure B8.** Thermal conductivities from Hole-in-Rock 1.

**Table B8.** Thermal conductivity measurements for Hole-in-Rock 1*

| Depth (m) | Thermal Conductivity[m] ($Wm^{-1}K^{-1}$) |
|---|---|
| 198 | 2.57 |
| 472 | 3.08 |
| 646 | 2.79 |
| 719 | 3.09 |
| 835 | 2.70 |
| 835 | 3.18 |
| 933 | 3.49 |
| 1070 | 2.93 |
| 1234 | 4.44 |
| 1350 | 3.31 |
| 1469 | 2.91 |
| 1533 | 3.73 |
| 1646 | 2.99 |
| 1807 | 3.34 |
| 1951 | 3.64 |
| 2131 | 3.39 |
| 2179 | 3.73 |
| 2240 | 3.16 |
| 2304 | 3.36 |
| 2365 | 3.22 |
| 2426 | 2.31 |
| 2487 | 2.79 |
| 2542 | 2.34 |
| 2609 | 2.81 |
| 2670 | 2.99 |
| 2731 | 3.05 |
| 2791 | 2.90 |
| 2847 | 5.60 |
| 2914 | 5.84 |
| 2975 | 6.15 |
| 3036 | 7.08 |
| 3088 | 6.44 |
| 3159 | 7.04 |
| 3222 | 4.90 |
| 3280 | 3.74 |
| 3344 | 2.80 |

*Thermal conductivity measured on divided bar. [m]Matrix conductivity.

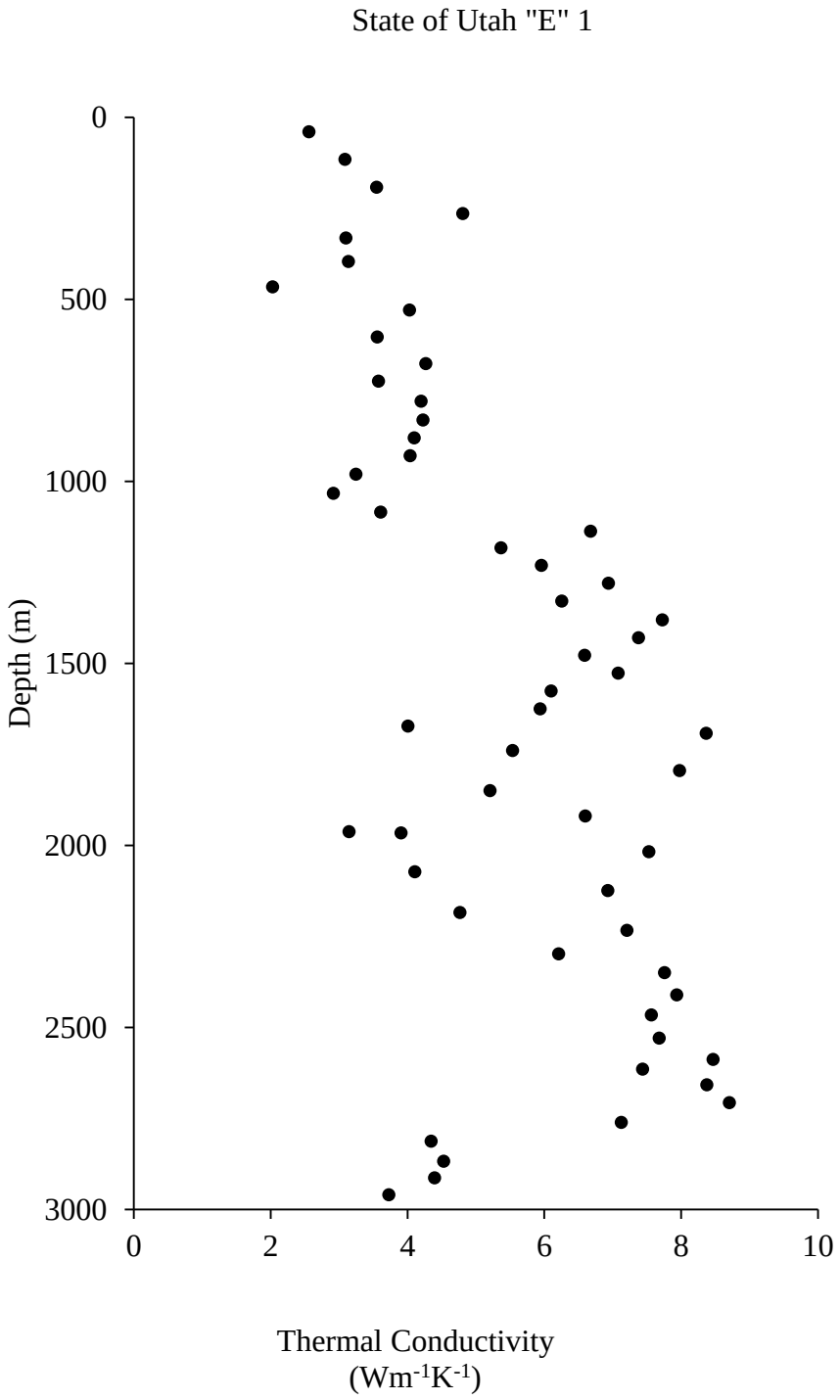


**Figure B9.** Thermal conductivities from State of Utah “E” 1.

**Table B9.** Thermal conductivity measurements for State of Utah "E" 1*

| Depth (m) | Thermal Conductivity[m] ($Wm^{-1}K^{-1}$) | Depth (m) | Thermal Conductivity[m] ($Wm^{-1}K^{-1}$) |
|---|---|---|---|
| 40 | 2.56 | 1966 | 3.91 |
| 116 | 3.09 | 2018 | 7.53 |
| 192 | 3.55 | 2073 | 4.11 |
| 265 | 4.81 | 2124 | 6.93 |
| 332 | 3.10 | 2185 | 4.77 |
| 396 | 3.14 | 2234 | 7.21 |
| 466 | 2.03 | 2298 | 6.21 |
| 530 | 4.03 | 2350 | 7.76 |
| 604 | 3.56 | 2411 | 7.94 |
| 677 | 4.27 | 2466 | 7.57 |
| 725 | 3.58 | 2530 | 7.68 |
| 780 | 4.20 | 2588 | 8.47 |
| 832 | 4.23 | 2615 | 7.44 |
| 881 | 4.10 | 2658 | 8.38 |
| 930 | 4.04 | 2707 | 8.71 |
| 981 | 3.25 | 2761 | 7.13 |
| 1033 | 2.92 | 2813 | 4.35 |
| 1085 | 3.61 | 2868 | 4.53 |
| 1137 | 6.68 | 2914 | 4.40 |
| 1183 | 5.37 | 2960 | 3.73 |
| 1231 | 5.96 | | |
| 1280 | 6.94 | | |
| 1329 | 6.26 | | |
| 1381 | 7.73 | | |
| 1430 | 7.38 | | |
| 1478 | 6.59 | | |
| 1527 | 7.08 | | |
| 1576 | 6.10 | | |
| 1625 | 5.94 | | |
| 1673 | 4.01 | | |
| 1692 | 8.37 | | |
| 1740 | 5.54 | | |
| 1795 | 7.98 | | |
| 1850 | 5.21 | | |
| 1920 | 6.60 | | |
| 1963 | 3.15 | | |

*Thermal conductivity measured on divided bar. [m]Matrix conductivity.

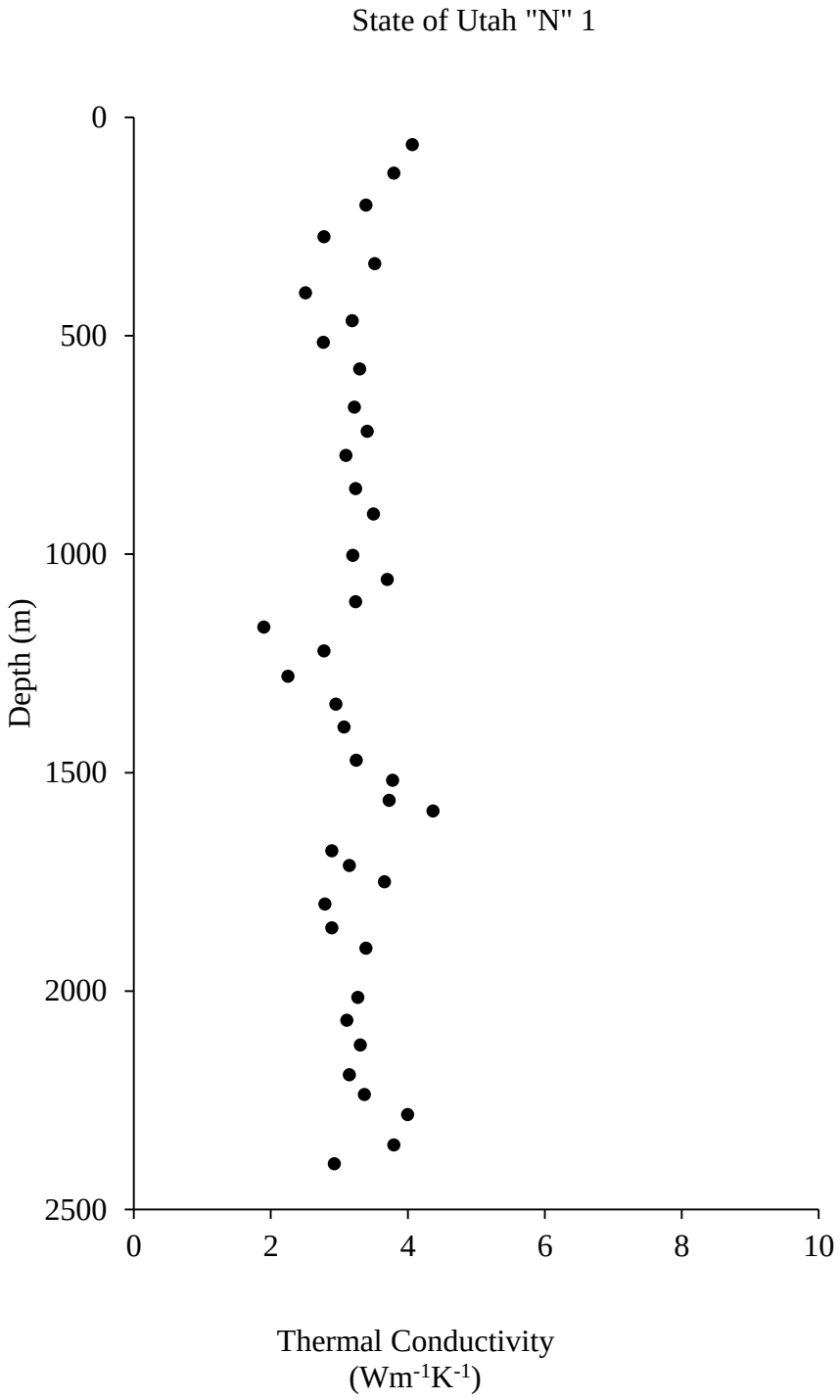


**Figure B9.** Thermal conductivities from State of Utah “N” 1.

**Table B10.** Thermal conductivity measurements for State of Utah "N" 1*

| Depth (m) | Thermal Conductivity[m] ($Wm^{-1}K^{-1}$) | Depth (m) | Thermal Conductivity[m] ($Wm^{-1}K^{-1}$) |
|---|---|---|---|
| 63 | 4.07 | 2192 | 3.15 |
| 128 | 3.80 | 2237 | 3.37 |
| 201 | 3.39 | 2283 | 4.00 |
| 274 | 2.78 | 2353 | 3.80 |
| 335 | 3.52 | 2396 | 2.93 |
| 402 | 2.51 | | |
| 466 | 3.19 | | |
| 515 | 2.77 | | |
| 576 | 3.30 | | |
| 664 | 3.22 | | |
| 719 | 3.41 | | |
| 774 | 3.10 | | |
| 850 | 3.24 | | |
| 908 | 3.50 | | |
| 1003 | 3.20 | | |
| 1058 | 3.70 | | |
| 1109 | 3.24 | | |
| 1167 | 1.90 | | |
| 1222 | 2.78 | | |
| 1280 | 2.25 | | |
| 1344 | 2.95 | | |
| 1396 | 3.07 | | |
| 1472 | 3.25 | | |
| 1518 | 3.78 | | |
| 1564 | 3.73 | | |
| 1588 | 4.37 | | |
| 1679 | 2.89 | | |
| 1713 | 3.15 | | |
| 1750 | 3.66 | | |
| 1801 | 2.79 | | |
| 1856 | 2.89 | | |
| 1902 | 3.39 | | |
| 2015 | 3.27 | | |
| 2067 | 3.11 | | |
| 2124 | 3.31 | | |

*Thermal conductivity measured on divided bar. [m]Matrix conductivity.

**References**


Beardsmore, G. R., and J. P. Cull (2001), *Crustal Heat Flow: A Guide to Measurement and Modeling*, Cambridge University Press, Cambridge.

Bodell, J. M., and D. S. Chapman (1982), Heat flow in the north-central Colorado Plateau, *Journal of Geophysical Research*, *87*(B4), 2869, doi:10.1029/JB087iB04p02869.

Chapman, D. S. (1976), Heat flow and heat production in Zambia, 94 pp., University of Michigan.

Chapman, D. S., T. H. Keho, M. S. Bauer, and M. D. Picard (1984), Heat flow in the Uinta Basin determined from bottom hole temperature (BHT) data, *Geophysics*, *49*(4), 453–466, doi:10.1190/1.1441680.

Deming, D., and D. S. Chapman (1988), Inversion of bottom-hole temperature data: The Pineview field, Utah-Wyoming thrust belt, *Geophysics*, *53*(5), 707, doi:10.1190/1.1442504.

Henrickson, A. (2000), New Heat Flow Determinations from Oil and Gas wells in the Colorado Plateau and Basin and Range of Utah, 70 pp., University of Utah.

Moran, K. J. (1991), Shallow Thermal Regime at the Jordanelle Dam Site, Central Rocky Mountains, Utah, 141 pp., University of Utah.

Powell, W. G. (1997), Thermal State of the Lithosphere in the Colorado Plateau-Basin and Range Transition Zone, Utah, 232 pp., University of Utah.

Pribnow, D. F. C., and J. H. Sass (1995), Determination of thermal conductivity for deep boreholes, *Journal of Geophysical Research*, *100*(B6), 9981, doi:10.1029/95JB00960.

Sass, J. H., A. H. Lachenbruch, R. J. Munroe, G. W. Greene, and T. H. Moses (1971), Heat flow in the western United States, *Journal of Geophysical Research*, *76*(26), 6376–6413, doi:10.1029/JB076i026p06376.